

**Magnetic-field-induced magnetism and thermal stability of carbides $\text{Fe}_{6-x}\text{Mo}_x\text{C}$
in molybdenum-containing steels**

T.P. Hou,^{a*} Y. Li,^a K.M. Wu,^{a*} M.J. Peet,^b C.N. Hulme-Smith,^b and L. Guo^b

^a*The State Key Laboratory for Refractories and Metallurgy, Hubei Province Key Laboratory of Systems Science in Metallurgical Process, Hubei Collaborative Innovation Center for Advanced Steels, International Research Institute for Steel Technology, Wuhan University of Science and Technology, Wuhan 430081, China*

^b*Department of Materials Science and Metallurgy, University of Cambridge, UK*

*Corresponding author. Tel.: +86 27 68862772; Fax: +86 27 68862606; *E-mail address:* houtingping@wust.edu.cn;

*Corresponding author. Tel.: +86 27 68862772; Fax: +86 27 68862606; *E-mail address:* wukaiming@wust.edu.cn; 1052516931@qq.com

Abstract

A hybrid method combining first-principles calculations and Weiss molecular field theory with thermodynamic data has been implemented to explore the origin of magnetic-field-induced precipitation behaviors for alloy carbides. The paramagnetic Mo atom disturbed the order of magnetic moment and resulted in a decrease in the Curie temperature for alloy carbide $\text{Fe}_{6-x}\text{Mo}_x\text{C}$. The temperature dependence of magnetic moment and saturation magnetization of Fe atoms at different Wyckoff positions, as well as the saturation or induced magnetization of $\text{Fe}_{6-x}\text{Mo}_x\text{C}$, decreased with increasing temperature. The higher Fe content and external magnetic field greatly increased the magnetization of alloy carbides. Two kinds of stella quadrangula lattices were employed to account for the total magnetism which was derived from the contribution of different Wyckoff sites of Fe atoms and Fe-C distances. The calculated total free energy taking into account magnetic field, temperature and composition was sufficient to provide quantitative agreement with experiment. The investigation of the effects of external field on the carbide precipitation behaviors led to a better understanding of the magnetic-field-induced phase transformation mechanism in heat resistant steels.

Keywords: Steels; Carbide; High magnetic field; Magnetism; Stability

1. Introduction

It is generally considered that a high magnetic field has a significant influence on the phase transformation of ferromagnetic materials. So far, the research on magnetic field related topics focuses on the following aspects: martensite [1-3], bainite [4], ferrite [5] and pearlite [6] transformations, the nucleation and growth of cementite [7], and carbide precipitation [8]. Recently more attention has been paid to the precipitation sequence and growth behavior of iron carbides which is influenced by high magnetic fields [9,10]. Under normal circumstances it is generally believed that the alloy carbides are paramagnetic phases and the external field has almost no influence on them. However, preliminary results have revealed that the precipitation sequence and substitutional solute atom concentration of alloy carbides M_6C and $M_{23}C_6$ are changed by high magnetic fields [8,11,12]. Magnetic-field-induced precipitation in alloys, especially for steels used under the extreme conditions of high magnetic field and intermediate temperature, is an important scientific and technological interest. Improved descriptions of the Plasma Wall Interaction in a magnetic confinement Tokamak [13] is generally considered necessary to solve the key magnetism problem in International Thermonuclear Experimental Reactor. It is the basis for the development of fusion energy, in which steels work under the extreme conditions of high magnetic field and temperature. Driven by the technical demands, magnetism research appears to be highly extended and deepened, in particular, the twofold effects of temperature and magnetic field. Many works are concentrated on experimental phenomena to clarify the effect of the magnetic field on microstructure. However, there are still many theoretical issues to be explored, especially for alloy carbides, so as to further understand the coupling effects of the external field-dependence and temperature-dependence.

In solid state physics, magnetism is one of the most intriguing features of matter. A number of

approaches based on consideration of quantum mechanics have been used to develop models describing magnetic effects. Based on the Boltzmann distribution, the magnetic susceptibility for cementite has been obtained using first principle density functional theory [14]. The itinerant electron model [15], dealing with almost free electrons, is intrinsically close to reality in most cases, but it does not provide any simple model from which first-principles calculations can be made. In view of this drawback, magnetic properties can be interpreted on the basis of the Weiss model [16]. The Weiss model is applicable to electrons that are localized within a lattice of positive ions.

M_6C carbide in Fe-C-Mo alloy system belongs to the $Fd\bar{3}m$ space group [17]. There are three kinds of known structures Fe_2Mo_4C [17], Fe_3Mo_3C [18] and Fe_4Mo_2C [19]. M_6C (Fe_2Mo_4C , Fe_3Mo_3C and Fe_4Mo_2C) is the predominant precipitated carbide in molybdenum-containing alloys under high magnetic field [20,21]. The Gibbs free energy (ΔG), which determines the phase stability, is closely related to the magnetization and magnetic susceptibility in ferromagnetic and paramagnetic substances, respectively. The present work attempts to investigate quantitatively the magnetism characteristics of the alloy carbides $Fe_{6-x}Mo_xC$. Firstly, the first-principles calculations are used in conjunction with the Weiss model to determine simultaneously the magnetic moment and the temperature dependence of magnetization in alloy carbides $Fe_{6-x}Mo_xC$. Then, we compare the contributions of the magnetic and thermal influences on the stability with calculations using a mixed description of magnetic and non-magnetic effects.

2. Previous experimental results

The experimental procedures and materials have been described in detail in our previous works [8,21,22]. A magnetic field of 12 Tesla was applied during quench-tempering and austenite-to-bainite transformation heat treatments of Fe-0.28C-3.0Mo alloy. The magnetic field effectively promoted the precipitation of the alloy carbide $(Fe, Mo)_6C$. The results are listed in

Table 1. We have discussed the effect of high magnetic field on the precipitation sequence based on the magnetic free energy and precipitation morphology at a fixed magnetic field strength (12 T) [21]. It is, however, difficult to experimentally distinguish different kinds of $\text{Fe}_{6-x}\text{Mo}_x\text{C}$ from the morphology because alloy carbides $\text{Fe}_{6-x}\text{Mo}_x\text{C}$ (Fig. 1) remain similarly globular whether it is under a 12 T magnetic field or not, especially in the later stages of isothermal transformation. $\text{Fe}_{6-x}\text{Mo}_x\text{C}$ magnetism indeed varies with the Fe or Mo atom concentration under high magnetic field [22]. It is therefore expected that a systematic theoretical simulation should provide more sufficient magnetic data of alloy carbides. The previous main theoretical considerations were emphasized on the change of the magnetic free energy with temperature [21]. In fact, the influencing factors including the quantum number, Curie temperature and external field intensity, which are closely related to magnetic free energy change, should be considered. Although magnetic free energy was found to provide an excellent description of the available experimental data, it did not capture the combined effects of the chemical composition, temperature and external field. The coupling of thermal free energy and magnetic free energy can provide a more accurate description and proper interpretation for magnetic-induced precipitation behaviors.

3. Calculation Methods

3.1 First-principles calculations of different alloy carbides

The total magnetic moments per unit cell of transition carbide have been obtained using first-principles calculations. The all-electron full-potential linearized augmented plane wave method was used as embodied in the WIEN2K code [23]. The exchange-correlation potential was calculated using the generalized gradient approximation via the scheme of Perdew-Burke-Ernzerhof 96 [24]. The electronic wave functions were sampled with 47, 72 and 72 k-points in the irreducible Brillouin zone of $\text{Fe}_2\text{Mo}_4\text{C}$, $\text{Fe}_3\text{Mo}_3\text{C}$ and $\text{Fe}_4\text{Mo}_2\text{C}$, respectively. The sphere radii (muffin tin) were

$R_{MT}=2.22, 2.10$ and 1.86 a.u. for iron, molybdenum and carbon atoms, respectively. The use of the full potential ensured that the calculation was completely independent of the choice of the sphere radii. Different plane waves were tested, e.g. 2433~2453 grids for $Fe_{6-x}Mo_xC$. Fe_4Mo_2C is less commonly observed in steel and, there is no reliable reference for the details of structure data. In this work, the Fe, Mo1 and Mo2 Wyckoff sites in Fe_2Mo_4C were correspondingly replaced with Mo, Fe2 and Fe1 sites to obtain the structure of Fe_4Mo_2C .

3.2 Weiss molecular field theory and the iterative process of calculation for alloy carbide M_6C

The theory of paramagnetism, originally developed by Langevin (1905) [25] and extended by Weiss (1907) [26] to include ferromagnetism, led to expressions giving the variation of magnetization (M) with temperature above and below the Curie point. The cubic η -carbide-type structure M_6C has been reported [20,27]. The calculated magnetic moments from the first-principle calculation at 0 K, 0 Pa were considered as one of the input parameters in the Weiss molecular field theory [28]. Weiss speculated that spins are aligned by a molecular field in ferromagnetic materials and the field is proportional to the magnetic moment of materials. The theory is effective for clarifying the origin of ferromagnetism but short range ordering of spins is not considered. The iterative process on the magnetization calculation is described as follows:

The temperature range is given as 0 K to T_{max} and divided into n steps. The temperature at i^{th} step can be obtained by equation (1):

$$T_i = T_{i-1} + \frac{T_{max}}{n} \quad (1)$$

When n is infinite, $\frac{T_{max}}{n} \rightarrow 0$ and $T_i \approx T_{i-1}$. A magnetic field B is applied to an ensemble of N atoms per unit volume, each having a magnetic moment m . The saturation magnetization at 0 Pa and 0 K is defined as $M_0 = Nm = Nj\mu_B g$ with the Landé factor g , Bohr magneton μ_B and quantum number j .

The temperature-dependence magnetization M can be expressed as in equation (2):

$$M_i = NmB_j \left[\frac{m(B + \lambda M_{i-1})}{kT_i} \right] \quad (2)$$

where M_i is the magnetization at the temperature T_i , $B_j \left[\frac{m(B + \lambda M_{i-1})}{kT_i} \right]$ the Brillouin function, k the Boltzman constant and λ is the molecular field constant.

4. Results and discussion

4.1 The quantum numbers for alloy carbides $\text{Fe}_{6-x}\text{Mo}_x\text{C}$

Metallic compounds with similar composition and structure may be considered as having similar magnetic properties, as reported between $\eta\text{-Fe}_2\text{C}$ and $\varepsilon\text{-Fe}_2\text{C}$ [29] and between $\chi\text{-Fe}_5\text{C}_2$ and $\theta\text{-Fe}_3\text{C}$ [30]. Therefore, it has been reasonably deduced that alloy carbides $\text{Fe}_{6-x}\text{Mo}_x\text{C}$ ($\text{Fe}_2\text{Mo}_4\text{C}$, $\text{Fe}_3\text{Mo}_3\text{C}$ and $\text{Fe}_4\text{Mo}_2\text{C}$) have similar magnetic properties. For alloy carbides $\text{Fe}_{6-x}\text{Mo}_x\text{C}$, the overall magnetic moments are mainly determined by the magnetic moments of their iron atoms due to the paramagnetism of the Mo atoms. The quantum number j is closely connected to the magnetization M .

Firstly, we concentrate the investigation on the treatment of the magnetic properties of iron. The saturation magnetization M_0 is almost entirely determined by the strongly localized 3d electrons and is, therefore, given by the total magnetization scaled by the number of atoms and the Landé factor $g \approx 2$. A significant step toward quantitative agreement with experiment has been made by establishing a simple formula in equation (3) describing the temperature dependence of the spontaneous magnetization of iron [31]. This fulfills Bloch's famous $T^{3/2}$ law for low temperatures and was empirically derived from a detailed analysis of the corresponding experimental data for several ferromagnetic systems.

$$M_i(T) = [1 - s(T/T_c)^{3/2} - (1-s)(T/T_c)^4]^{1/3} \quad (3)$$

where s (or j) and the Curie temperature (T_c) are 0.35 and 1044 K, respectively. The obtained results of the magnetization (thin solid line) perfectly describe the experimental data (hollow circle) [32], as shown in Fig. 2. However, the formula is not capable of taking an applied magnetic field into account. The random phase approximation (RPA), which does consider the magnetic excitation, is known to give a more accurate Curie temperature [33]. However, the temperature-dependent magnetization given by RPA in Fig. 2 (dotted line) strongly deviates from the experimental data and is not sufficient to account for the magnetic contribution to the free energy [34].

Secondly, in order to reconcile the experimental results [32] and the requirement of the magnetic free energy calculation [34], simple molecular field theory was used with $j=1$ to find the magnetization for pure iron, as shown in Fig. 2 (thick solid line). Similar to pure iron, j was also set to 1 for the alloy carbide, as the contribution from iron atoms dominates its magnetization and magnetic free energy.

4.2 The interaction between high magnetic field and Curie temperature

In the absence of an external magnetic field, T_c is defined as the temperature at which the magnetization equals zero on the magnetization-temperature curve. T_c can be shifted by imposing an external magnetic field and/or altering the composition. Previous work has revealed that T_c depends not only on the magnetization but also on the magnetic exchange interaction coefficients which is well connected with composition [35]. T_c is greatly raised by high magnetic fields in Fe-X alloy systems [36,37]. To our knowledge, there is no previous work in which the Curie temperature for M_6C has been determined. However, previous experimental results did demonstrate that the precipitation of M_6C carbide was affected by high magnetic field even at high temperatures (610°C) [8].

In this study, T_c is obtained by the following equation (4):

$$\frac{\partial^2 M(x, B)}{\partial T^2} = 0 \quad (4)$$

where x is the concentration of Mo atoms in $\text{Fe}_{6-x}\text{Mo}_x\text{C}$. Fig. 3 shows that T_c increases with increasing external magnetic field strength from 0 to 20 T. The higher external magnetic fields make the exchange interaction between parallel magnetic moments stronger [36]. Furthermore, it is well known that the iron atom carries a higher magnetic moment due to the spin of its unpaired 3d electrons. The influence of the magnetic field on the Curie temperature mainly depends on the Fe concentration in $\text{Fe}_{6-x}\text{Mo}_x\text{C}$ carbides. The degree to which the Curie temperature is influenced by the external field for the three alloy carbides is in the sequence of $\text{Fe}_4\text{Mo}_2\text{C} > \text{Fe}_3\text{Mo}_3\text{C} > \text{Fe}_2\text{Mo}_4\text{C}$. In other words, the increase in Fe concentration obviously changes the order of magnetic moment and results in the decrease of T_c .

4.3 Comparison of Fe atom magnetic moment in different Wyckoff positions of alloy carbides $\text{Fe}_{6-x}\text{Mo}_x\text{C}$ with pure Fe at 0 K, 0 Pa

The knowledge of partial magnetic moments has played a critical role in developing theories and models of ferromagnetic behavior. The magnetic moments of Fe atom in Fe, $\text{Fe}_2\text{Mo}_4\text{C}$, $\text{Fe}_3\text{Mo}_3\text{C}$ and $\text{Fe}_4\text{Mo}_2\text{C}$ alloy carbides were calculated from the first-principles calculations at 0 K, 0 Pa, as shown in Fig. 4. It shows the average local magnetic moments of distinct Fe atoms at different Wyckoff positions (48f, 32e and 16d). The calculated local magnetic moment of Fe in $\text{Fe}_2\text{Mo}_4\text{C}$ (in Table 2), $\text{Fe}_3\text{Mo}_3\text{C}$ and $\text{Fe}_4\text{Mo}_2\text{C}$ alloy carbides was smaller than that of the pure Fe. The magnetic moment of Fe decreased with the increase of Mo content from $\text{Fe}_4\text{Mo}_2\text{C}$, $\text{Fe}_3\text{Mo}_3\text{C}$ to $\text{Fe}_2\text{Mo}_4\text{C}$. For $\text{Fe}_4\text{Mo}_2\text{C}$, however, the magnetic moment of Fe atom in 16d remarkably deviated from the other values, as shown in Fig. 4. Below, we discuss the magnetic features of the three phases in detail.

4.4 The relationship among the magnetic moment with the Pseudo-SQ lattice, Wyckoff

positions and Fe-C bond distances in alloy carbides

In the structure of $\text{Fe}_3\text{Mo}_3\text{C}$, Fe, Mo and C atoms occupy the Wyckoff positions 16d/32e, 48f and 16c, respectively. Focusing on Fe, which is expected to dominate the magnetic properties of the system, the 16d/32e sites form a three-dimensional network of stella quadrangula (SQ) lattice [38]. SQ is a polyhedron with each face of a tetrahedron composed of 32e atoms which is capped with another tetrahedron whose extra apex is 16d atoms. Different from the SQ lattice in $\text{Fe}_3\text{Mo}_3\text{C}$, the Wyckoff positions 16d/32e are occupied by Mo or Fe atoms for $\text{Fe}_2\text{Mo}_4\text{C}$ and $\text{Fe}_4\text{Mo}_2\text{C}$. This kind of three-dimensional network is called pseudo-SQ lattice in the present work. Fig. 5 shows the SQ lattice of $\text{Fe}_3\text{Mo}_3\text{C}$ and the pseudo-SQ lattices for $\text{Fe}_2\text{Mo}_4\text{C}$ and $\text{Fe}_4\text{Mo}_2\text{C}$ carbides. The magnetic moment roughly equals $1.84 \mu_B$ per SQ lattice in Fig. 5(b) by considering the contribution of the Fe atoms in 16d and 32e sites. Different from $\text{Fe}_3\text{Mo}_3\text{C}$, the magnetic moment in the pseudo-SQs in Fig. 5 (a and c) results from the cooperation of Fe and Mo atoms. The magnetic moments of Mo atoms in $\text{Fe}_2\text{Mo}_4\text{C}$ and $\text{Fe}_4\text{Mo}_2\text{C}$ are $-0.093 \mu_B$ and $-0.183 \mu_B$, respectively. Correspondingly, the magnetic moments in pseudo-SQ lattice in $\text{Fe}_2\text{Mo}_4\text{C}$ and $\text{Fe}_4\text{Mo}_2\text{C}$ are $1.24 \mu_B$ and $0.64 \mu_B$, respectively. The order of increasing magnetic moment is $\text{Fe}_4\text{Mo}_2\text{C}$, $\text{Fe}_2\text{Mo}_4\text{C}$ and $\text{Fe}_3\text{Mo}_3\text{C}$. However, experimentally the effect of magnetic field strength on $\text{Fe}_4\text{Mo}_2\text{C}$ is much more significant than that of $\text{Fe}_2\text{Mo}_4\text{C}$ or/and $\text{Fe}_3\text{Mo}_3\text{C}$ at an intermediate temperature during the tempering of Fe-C-Mo alloy [22].

Apart from the lattice types, the different Fe Wyckoff positions and near-neighbor Fe-C bonds simultaneously play an important role in determining the magnetism of alloy carbides. As shown in Table 3, the near-neighbor Fe-C bond lengths for the Fe atoms in 48f and 16d sites are about 2.12 \AA (Table 3) and 3.93 \AA for $\text{Fe}_4\text{Mo}_2\text{C}$ respectively. The Fe atoms in 48f sites have a local magnetic moment of about $2.06 \mu_B$, which is larger than that for Fe in 16d sites ($0.83 \mu_B$) (Fig. 4).

Furthermore, in $\text{Fe}_4\text{Mo}_2\text{C}$, $\text{Fe}_3\text{Mo}_3\text{C}$ and $\text{Fe}_2\text{Mo}_4\text{C}$, the nearest-neighbor Fe-C bond distances decrease with the higher Fe atom concentration, which corresponds to the higher magnetic moment value, as displayed in Table 3. In other words, the reduction in the Fe-C distances upon the removal of Mo atom would indicate the increased ferromagnetism. These results agree with the general conception that strong Fe-C hybridization reduces the local moment of Fe atoms [39,40]. It is mainly because that the magnetic moment of C also directly influences the magnetism of Fe atoms according to the polarization [41].

4.5 Magnetic-field-induced variation of the magnetic moment of Fe atom

The magnetic moment transition of both iron atoms 8d and 4c sites from the ferromagnetic to the non-magnetic state occurs at high pressure (e.g. 55 GPa) for Fe_3C carbide [42]. Under high external magnetic field, the variation of saturation magnetization was calculated for Fe atoms in 16d and 48f sites in $\text{Fe}_4\text{Mo}_2\text{C}$ with different temperatures and magnetic field strengths of 0, 6, 12 and 18 T by means of molecular field theory, as shown in Fig. 6. Similar to the trend in magnetization for iron in Fig. 2, the saturation magnetization of different Wyckoff positions 48f or 16d of Fe atom in $\text{Fe}_4\text{Mo}_2\text{C}$ decreases with increasing temperature under a fixed magnetic field strength. The saturation magnetization of both types of site increases with increasing external magnetic field strength at a given temperature. This is because the magnetic moment of ferromagnetic materials will be aligned in the direction of external field. The increase of parallel magnetic moment promotes the exchange interaction and therefore increases the saturation magnetization.

4.6 Magnetic-field-induced magnetization of alloy carbides

The results of first-principles calculations to derive the variation of saturation magnetization with the number of electrons per atom for $\text{Fe}_{6-x}\text{Mo}_x\text{C}$ carbides at 0 K and 0 Pa are shown in Fig. 7. The electron number per atom for M_6C varies from 26 (pure Fe) to 42 (pure Mo). The number of

electrons per atom is 30.05 and 33.04 for the experimental concentration of substitutional solute atoms $\text{Fe}_{4.68}\text{Mo}_{1.32}$ and $\text{Fe}_{3.36}\text{Mo}_{2.64}$ [22], respectively. With the increase of Mo content, the saturation magnetization of $\text{Fe}_4\text{Mo}_2\text{C}$, $\text{Fe}_3\text{Mo}_3\text{C}$ and $\text{Fe}_2\text{Mo}_4\text{C}$ decreases due to the paramagnetism of the Mo atom. Furthermore, the higher Fe content corresponds to a higher saturation magnetization. For the three carbides the saturation magnetization results from the first-principles calculations are in the sequence of $\text{Fe}_4\text{Mo}_2\text{C} > \text{Fe}_3\text{Mo}_3\text{C} > \text{Fe}_2\text{Mo}_4\text{C}$ at 0 K and 0 Pa.

The temperature dependence of induced magnetization with different external magnetic fields in $\text{Fe}_{6-x}\text{Mo}_x\text{C}$ was calculated from Weiss theory and shown in Fig. 8. It can be seen that the magnetization was remarkably decreased with increasing temperature, and the magnetization curves shifted to higher temperature with the increase of external magnetic field strength, which means the external magnetic field can improve the ferromagnetism of M_6C alloy carbides. For each phase, the magnetization increased with increasing external field strength. The magnetization influenced by high magnetic field of three alloy carbides was in the same sequence as that in the 0 K and 0 Pa. In summary, higher Fe content and stronger external field can greatly increase the magnetization.

4.7 Magnetic contribution to Gibbs free energy

Several studies [43-45] indicated that if some Cr or Mo atoms are replaced by Fe, the carbide will have higher formation energy which is closely related to its stability. Substitution of an additional Mo atom into (Ti, M)C carbide is energetically unfavorable because of the higher formation energy [43]. Widom et al. reported that the stability in Cr_{23}C_6 prototype can be improved by Cr atom occupying the 8c site [44]. Xie et al. [45] employing Morse potentials showed that the formation energy of $\text{Cr}_x\text{Fe}_{23-x}\text{C}_6$ increases with increasing Fe content. However, how a high magnetic field influences the molybdenum-containing carbide is still to be revealed.

The magnetic Gibbs free energy related to the stability is lowered in relation to the

magnetization and external field strength. The relatively higher magnetization should be supposed to easily reach saturation in a high magnetic field. The magnetization of alloy carbide $\text{Fe}_4\text{Mo}_2\text{C}$ was higher than that of $\text{Fe}_3\text{Mo}_3\text{C}$ and $\text{Fe}_2\text{Mo}_4\text{C}$. For the three alloy carbides ($\text{Fe}_2\text{Mo}_4\text{C}$, $\text{Fe}_3\text{Mo}_3\text{C}$ and $\text{Fe}_4\text{Mo}_2\text{C}$), the higher Fe atom content leads to a remarkable decrease in the magnetic Gibbs free energy ($\Delta G_M(T, B) = -\mu_0 \int_0^B \vec{M} \cdot d\vec{B}$), as shown in Fig. 9. This implies that the magnetic field has an obvious influence on the higher Fe-containing alloy carbide, which is in agreement with experimental results for the Fe-C-Mo alloy [20].

4.8 The thermal and magnetic free energy for M_2C , M_3C and M_6C

The thermal Gibbs free energies of M_2C , M_3C and M_6C at constant pressure have been calculated using MTDATA with TCAB database for steels version 1.0 [46]. MTDATA is a thermodynamic software which can predict the phases forming at equilibrium in multi-components and multi-phases alloy systems. It is based upon critically assessed thermodynamic data for simpler sub-systems, and uses a very robust algorithm (STAGE_1). Gibbs free energy of different phases can be obtained by varying a single variable between two values (temperature, weight percent of a component ...) and plotting whichever other variable of interest as a function of the stepped one.

When magnetic field (12 T) is applied, the resulting free energy change $\Delta G_{total}(T, X, B)$ can be classified into two terms in equation (5): the thermal Gibbs free energy $\Delta G(T, X)$ which was determined using MTDATA software, and the magnetic Gibbs free energy $\Delta G_M(T, B)$, where X is the composition parameter of alloy carbides.

$$\Delta G_{total}(T, X, B) = \Delta G(T, X) + \Delta G_M(T, B) \quad (5)$$

The total Gibbs free energy change $\Delta G_{total}^{\gamma \rightarrow \alpha}(T, X, B) = 0$ as a function of temperature and magnetic field has been investigated and the result showed that the calculated γ/α transformation temperature in pure iron ($X = 0$) increased about 10 K with the 12 T magnetic field [47]. For alloy

carbides, the formation temperatures for M_2C , M_3C and M_6C increases by 3, 7.5 and 11 K, respectively, as shown in Table 4.

The major controlling factor R in equation (6) is used to express the percentage ratio of the magnetic free energy change $\Delta G_M(T, B)$ over the total energy change $\Delta G_{total}(T, X, B)$.

$$R = \frac{\Delta G_M(T, B)}{\Delta G_{total}(T, X, B)} \times 100\% \quad (6)$$

To better understand the role of the thermal and magnetic contributions to the free energy, we firstly consider Fe_2C , Fe_3C and Fe_3Mo_3C only. Up to a temperature of about 1000 K in Fig. 10, the percentage ratio R in equation (6) follows the sequence of $M_6C > M_2C \approx M_3C$. According to thermodynamics modelling predictions for equilibria between each carbide and austenite, M_6C first precipitates upon cooling at 1263 K. At lower temperature it coexists with austenite and is expected to dissolve at 1083 K. Within this temperature range of formation and dissolution, the R value is determined not only by the magnetic Gibbs free energy but also by the thermal free energy. R value increases with the temperature under 12 T magnetic field in Fig. 10. However, when the temperature is less than 1083 K the percentage ratio of the magnetic free energy to the total free energy for M_6C is almost 100% in Table 5. In contrast, M_2C and M_3C precipitate over a larger temperature range according to equilibrium thermodynamic modelling. Both R values are approximately less than 9% in the experimental temperature range (803 to 883 K). This indicates that the external field is a significant factor for determining the precipitation thermodynamics of M_6C . The result reveals an excellent agreement between the calculated magnetic contribution to the precipitation of M_6C and the corresponding experimental data in Table 1. Therefore, compared with M_2C and M_3C , the influence of temperature and magnetic field on Gibbs free energy is most remarkable for the alloy carbide M_6C .

5. Conclusions

The influence of high magnetic field on alloy carbide $\text{Fe}_{6-x}\text{Mo}_x\text{C}$ was investigated by means of a hybrid method combining the thermodynamic modelling software, first-principles calculations and Weiss molecular field theory. The magnetic-field-induced effect was analyzed by coupling the temperature, external magnetic field and composition. The relationship and possible correlations between magnetism and microstructure were investigated. The following conclusions have been drawn:

(1) External magnetic field and the higher Fe atom content in alloy carbides $\text{Fe}_{6-x}\text{Mo}_x\text{C}$ results in a remarkable increase of Curie temperature. The degree to which the alloy carbides are influenced by the external field is in the sequence of $\text{Fe}_4\text{Mo}_2\text{C} > \text{Fe}_3\text{Mo}_3\text{C} > \text{Fe}_2\text{Mo}_4\text{C}$.

(2) The total magnetic moment could be determined by the combined effect of the two kinds of SQ lattices, the different Wyckoff sites of Fe atoms and Fe-C distances.

(3) The magnetic moment and saturation magnetization of different Wyckoff positions of Fe atoms in $\text{Fe}_{6-x}\text{Mo}_x\text{C}$ decreased with increasing temperature. Each of a higher Fe content and a stronger external magnetic field could greatly increase the induced magnetization and thus, reduce the magnetic Gibbs free energy substantially.

(4) The thermal and magnetic field both influence the stability of alloy carbides, but magnetic field has a predominant contribution between 803 and 883 K for M_6C .

Acknowledgements

The authors are grateful to the financial support by National Natural Science Foundation of China (Grant Nos. 11404249 and U1532268), China Scholarship Council (Grant No. 201308420389), Science & Technology Research Program Young Talent Project of Education Bureau of Hubei Province of China (Grant No. Q20141101), State Key Laboratory of Refractories and Metallurgy (Wuhan University of Science and Technology (Grant No. G201504)) and Hubei

Province Key Laboratory of Systems Science in Metallurgical Process (Grant No. Y201404) as well as Hubei Province Natural Science Foundation (Grant No. 2013CFA131).

References

- [1] T. Kakeshita, K. Shimizu, T. Maki, I. Tamura, S. Kijima, Date M, Magnetoelastic martensitic transformation in an ausaged Fe-Ni-Co-Ti alloy, *Scripta Metall.* 19 (1985) 973-976.
- [2] D. San Martín, K.W.P. Aarts, P.E.J. Rivera-Díaz-del-Castillo, N.H. van Dijk, E. Brück, S. van der Zwaag, Isothermal martensitic transformation in a 12Cr-9Ni-4Mo-2Cu stainless steel in applied magnetic fields, *J. Magn. Magn. Mater.* 320 (2008) 1722-1728.
- [3] D. San Martín, N.H. van Dijk, E. Jiménez-Melero, E. Kampert, U. Zeitler, S. van der Zwaag, Real-time martensitic transformation kinetics in maraging steel under high magnetic fields, *Mater. Sci. Eng. A* 527 (2010) 5241-5245.
- [4] H. Ohtsuka, Effects of a high magnetic field on bainitic transformation in Fe-based alloys, *Mater. Sci. Eng. A* 438-440 (2006) 136-139.
- [5] G.H. Zhang, M. Enomoto, N. Hosokawa, M. Kagayama, Y. Adachi, Influence of magnetic field on ferrite transformation in a Fe-C-Mn alloy, *J. Magn. Magn. Mater.* 321 (2009) 4010-4016.
- [6] G.H. Zhang, M. Enomoto, Influence of magnetic field on isothermal pearlite transformation in Fe-C-Ni hypoeutectoid alloy, *Mater. Sci. Technol.* 26 (2010) 269-275.
- [7] Y.D. Zhang, N. Gey, C.S. He, X. Zhao, L. Zuo, C. Esling, High temperature tempering behaviors in a structural steel under high magnetic field, *Acta Mater.* 52 (2004) 3467-3474.
- [8] Z.N. Zhou, K.M. Wu, Molybdenum carbide precipitation in an Fe-C-Mo alloy under a high magnetic field, *Scripta Mater.* 61 (2009) 670-673.

- [9] Y.D. Zhang, X. Zhao, N. Bozzolo, C.S. He, L. Zuo, C. Esling, Low temperature tempering of a medium carbon steel in high magnetic field, *ISIJ. Int.* 45 (2005) 913-917.
- [10] T.P. Hou, Y. Li, J.J. Zhang, K.M. Wu, Effect of magnetic field on the carbide precipitation during tempering of a molybdenum-containing steel, *J. Magn. Magn. Mater.* 324 (2012) 857-861.
- [11] T.P. Hou, K.M. Wu, Alloy carbide precipitation in tempered 2.25 Cr–Mo steel under high magnetic field, *Acta Mater.* 61 (2013) 2016-2024.
- [12] T.P. Hou, K.M. Wu, The effect of high magnetic field on metal solute substitution in $M_{23}C_6$ alloy carbide, *Scripta Mater.* 67 (2012) 609-612.
- [13] J. Reece Roth, *Introduction to Fusion Energy*, Ibis Publishing, Charlottesville, Virginia, 1988.
- [14] Y.D. Zhang, H. Faraoun, C. Esling, L. Zuo, H. Aourag, Paramagnetic susceptibility of ferrite and cementite obtained from ab initio calculations, *J. Magn. Magn. Mater.* 299 (2006) 64-69.
- [15] D. Jiles, Quantum theory of magnetism, in: D. Jiles (First ed.), *Introduction to Magnetism and Materials*, Chapman and Hall, London, 1991, pp. 261-268.
- [16] D. Jiles, Magnetic order and critical phenomena, in: D. Jiles (Second ed.), *Introduction to Magnetism and Materials*, Chapman and Hall/CRC, London, 1998, pp. 228-232.
- [17] K. Kuo, The formation of η carbides properties, *Acta Metall.* 1 (1953) 301-304.
- [18] A. Silvia, S. Fernando, M. Eduardo, From nitrides to carbides: topotactic synthesis of the η -carbides Fe_3Mo_3C and Co_3Mo_3C , *Dalton Trans.* (2004) 2463-2468.
- [19] V. Adelsköld, A. Sundelin, A. Westgren, Carbide in kohlenstoffhaltigen Legierungen von Wolfram und Molybdän mit Chrom, Mangan, Eisen, Kobalt und Nickel, *Z. Anorg. Allg. Chem.* 212 (1933) 401-409.
- [20] T.P. Hou, Y. Li, K.M. Wu, Effect of high magnetic field on alloy carbide precipitation in an

Fe-C-Mo alloy, *J. Alloy. Compd.* 527 (2012) 240-246.

- [21] T.P. Hou, G. He, K.M. Wu, Y. Li, Magnetic-field-induced precipitation behavior of $(\text{Fe,Mo})_6\text{C}$ alloy carbides in a molybdenum alloyed steel, *Mater. Sci. Tech-Lond.* 30 (2014) 906-910.
- [22] T.P. Hou, Y. Li, Y.D. Zhang, K.M. Wu, Magnetic-field-induced precipitation behaviors of alloy carbides M_2C , M_3C and M_6C in a molybdenum-containing steel, *Metall. Mater. Trans. A* 45A (2014) 2553-2561.
- [23] P. Blaha, K. Schwarz, G.K.H. Madsen, D. Kvasnicka, J. Luitz, WIEN2K, an augmented plane wave + local orbital program for calculating crystal properties, Technical University at Wien, 2001.
- [24] J.P. Perdew, S. Burke, M. Ernzerhof, Generalized gradient approximation made simple, *Phys. Rev. Lett.* 77 (1996) 3865-3868.
- [25] P. Langevin, Magnetism and electron theory, *Ann. Chim. Phys.* 5 (1905) 70-127.
- [26] P. Weiss, The hypothesis of the molecular field and the property of ferromagnetism, *J. de Phys. Rad.* 6 (1907) 661-690.
- [27] D.V. Suetin, I.R. Shein, A.L. Ivanovskii, Structural, electronic and magnetic properties of η carbides ($\text{Fe}_3\text{W}_3\text{C}$, $\text{Fe}_6\text{W}_6\text{C}$, $\text{Co}_3\text{W}_3\text{C}$ and $\text{Co}_6\text{W}_6\text{C}$) from first principles calculations, *Physica B* 404 (2009) 3544-3549.
- [28] B.D. Cullity, Molecular field theory in: B.D. Cullity (First ed.), *Introduction to Magnetic Materials*, Addison-Wesley, Reading, Massachusetts, 1972, pp. 119-131.
- [29] G. Krauss, Tempering of Steel, in: G. Krauss, *Steels: Heat Treatment and Processing Principles*, Materials Park, Ohio, ASM International, 1990, pp. 205-262.
- [30] H.P.J. Wijn, Fe alloys and compounds, in: H.P.J. Wijn, *Magnetic Properties of Metals:*

D-elements, Alloys, and Compounds (Data in Science and Technology), Springer-verlag Berlin Heidelberg, 1991, pp. 151-155.

- [31] M.D. Kuz'min, Shape of temperature dependence of spontaneous magnetization of ferromagnets: quantitative analysis, *Phys. Rev. Lett.* 94 (2005) 107204-1-4.
- [32] J. Crangle, G.M. Goodman, The magnetization of pure iron and nickel, *Proc. Roy. Soc. Lond. A.* 321 (1971) 477-491.
- [33] J. Ruzs, L. Bergqvist, J. Kudrnovský, and I. Turek, Exchange interactions and Curie temperatures in Ni_{2-x}MnSb alloys: First-principles study, *Phys. Rev. B* 73 (2006) 214412-1-10.
- [34] F. Körmann, A. Dick, B. Grabowski, B. Hallstedt, T. Hickel, J. Neugebauer, Free energy of bcc iron: integrated ab initio derivation of vibrational, electronic, and magnetic contributions, *Phys. Rev. B* 78 (2008) 033102-1-4.
- [35] C. Takahashi, M. Ogura, H. Akai, First-principles calculation of the Curie temperature Slater-Pauling curve, *J. Phys. Condens. Matter.* 19 (2007) 365233-1-6.
- [36] X.J. Liu, Y.M. Fang, C.P. Wang, Y.Q. Ma, D.L. Peng, Effect of magnetic field on interfacial energy and precipitation behavior of carbides in reduced activation steels, *J. Alloy. Compd.* 459 (2008) 169-173.
- [37] H. Guo, M. Enomoto, Influence of magnetic fields on α/γ equilibrium in Fe-C(-X) alloys, *Mater. Trans. JIM.* 41 (2000) 911-916.
- [38] H. Nyman, S. Andersson, B.G. Hyde, M. O'Keeffe, The pyrochlore structure and its relatives, *J. Solid. State. Chem.* 26 (1978) 123-131.
- [39] C.M. Fang, M.A. van Huis, H.W. Zandbergen, Structural, electronic, and magnetic properties of iron carbide Fe₇C₃ phases from first-principles theory, *Phys. Rev. B* 80 (2009) 224108-1-9.

- [40] C.M. Fang, M.A. van Huis, M.H.F. Sluiter, H.W. Zandbergen, Stability, structure and electronic properties of γ -Fe₂₃C₆ from first-principles theory, *Acta Mater.* 58 (2010) 2968-2977.
- [41] C.T. Zhou, B. Xiao, J. Feng, J.D. Xing, X.J. Xie, Y.H. Chen, R. Zhou, First principles study on the elastic properties and electronic structures of (Fe, Cr)₃C, *Comp. Mater. Sci.* 45 (2009) 986-992.
- [42] S. Ono, K. Mibe, Magnetic transition of iron carbide at high pressures, *Phys. Earth. Planet. In.* 180 (2010) 1-6.
- [43] J.H. Jang, C.H. Lee, Y.U. Heo, D.W. Suh, Stability of (Ti, M)C (M= Nb, V, Mo and W) carbide in steels using first-principles calculations, *Acta Mater.* 60 (2012) 208-217.
- [44] M. Widom, M. Mihalkovic, Stability of Fe-based alloys with structure type C₆Cr₂₃, *J. Mater. Res.* 20 (2005) 237-242.
- [45] J.Y. Xie, N.X. Chen, L.D. Teng, S. Seetharaman, Atomistic study on the site preference and thermodynamic properties for Cr_{23-x}Fe_xC₆, *Acta Mater.* 53 (2005) 5305-5312.
- [46] MTDATA software, <http://www.msm.cam.ac.uk/phase-trans/mtdata/introduction.html>.
- [47] H.D. Joo, S.U. Kim, N.S. Shin, Y.M. Koo, An effect of high magnetic field on phase transformation in Fe-C system, *Mater. Lett.* 43 (2000) 225-229.

Figure 1

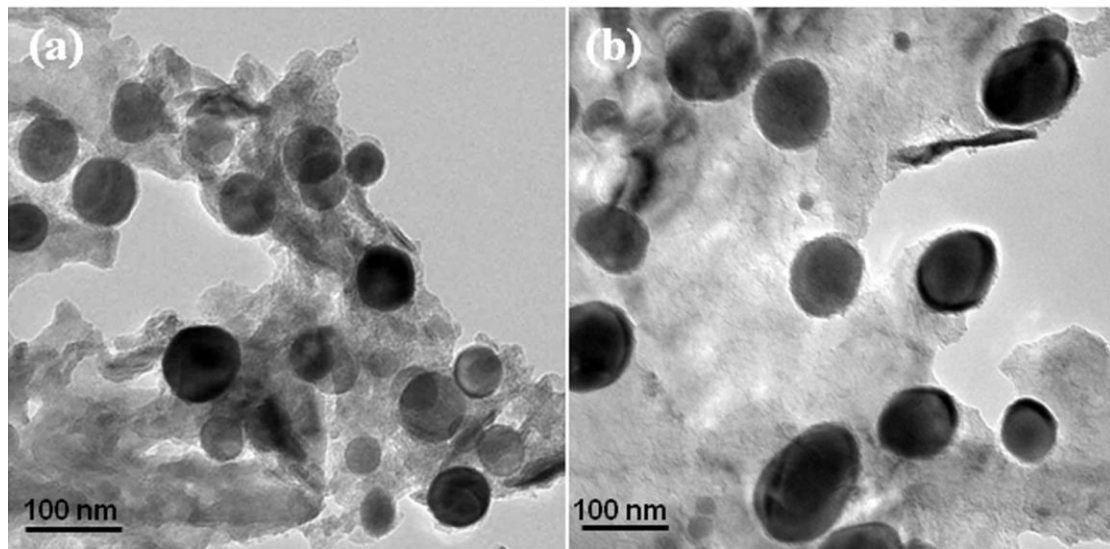


Fig. 1. Morphology of alloy carbides $(\text{Fe,Mo})_6\text{C}$ during isothermal holding at 570°C for 3600 s without (a) and with (b) the presence of 12 T magnetic field.

Figure 2

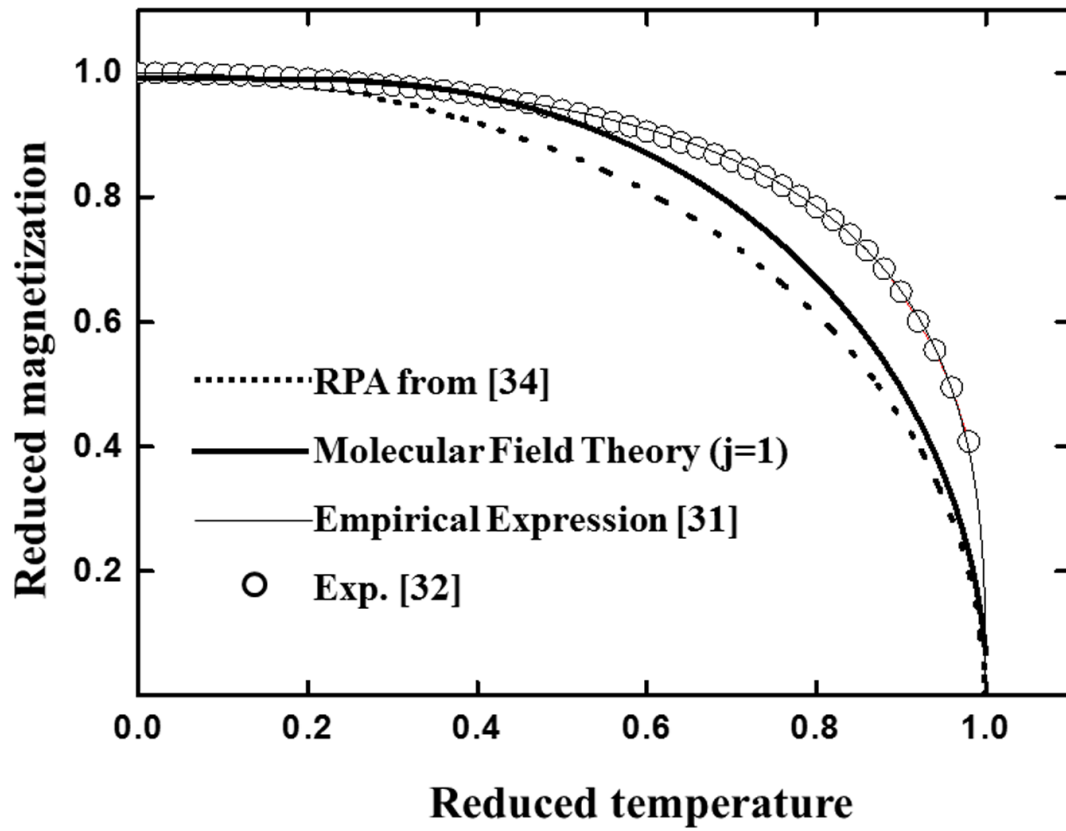


Fig. 2. Comparison of several theoretical approximations for the reduced magnetization (M/M_0) in comparison with experimental data. The results are plotted as a function of the reduced temperature (T/T_c).

Figure 3

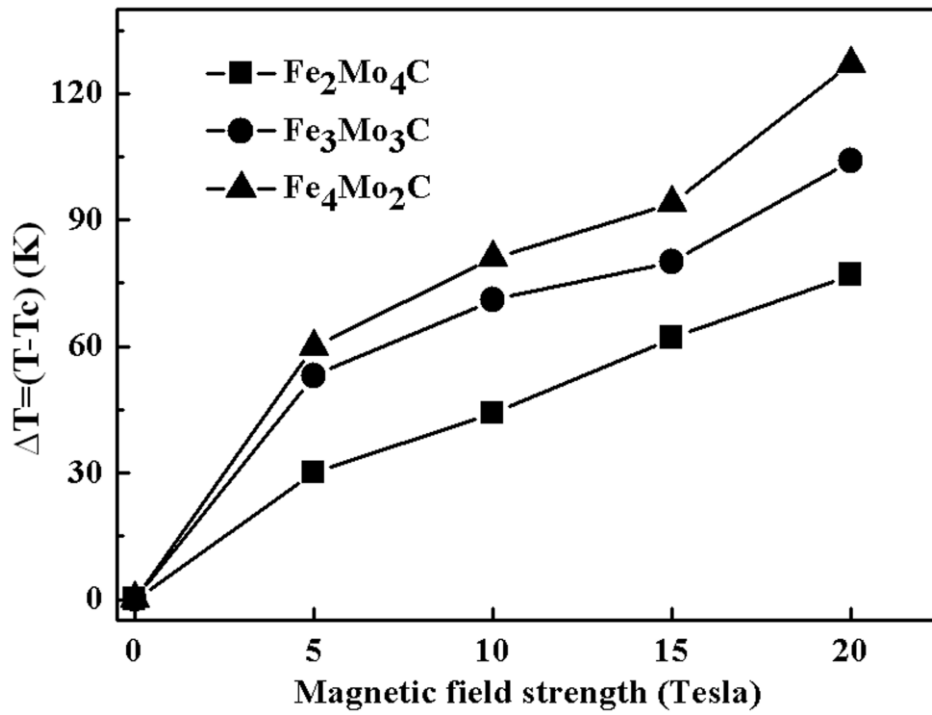


Fig. 3. Change of Curie temperature with various external magnetic fields for $\text{Fe}_{6-x}\text{Mo}_x\text{C}$.

Figure 4

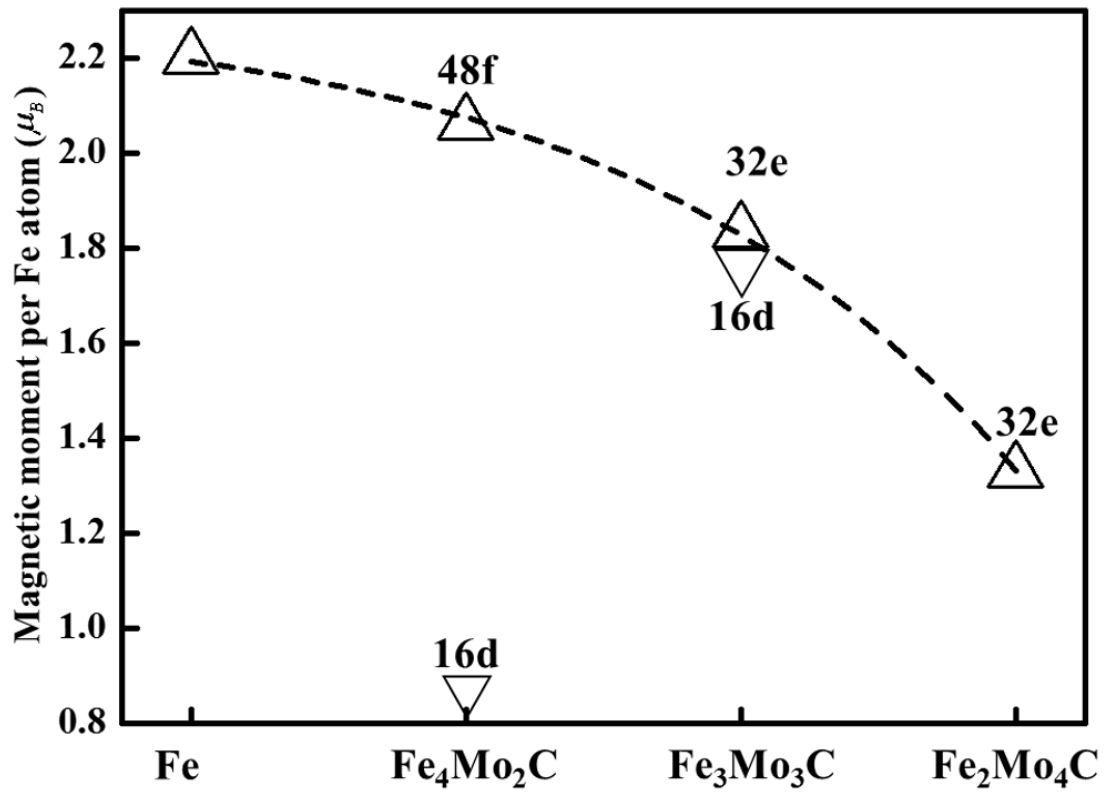


Fig. 4. Magnetic moments of Fe atoms calculated with the first-principles at 0 K and 0

Pa in the four phases: Fe, $\text{Fe}_2\text{Mo}_4\text{C}$, $\text{Fe}_3\text{Mo}_3\text{C}$ and $\text{Fe}_4\text{Mo}_2\text{C}$.

Figure 5

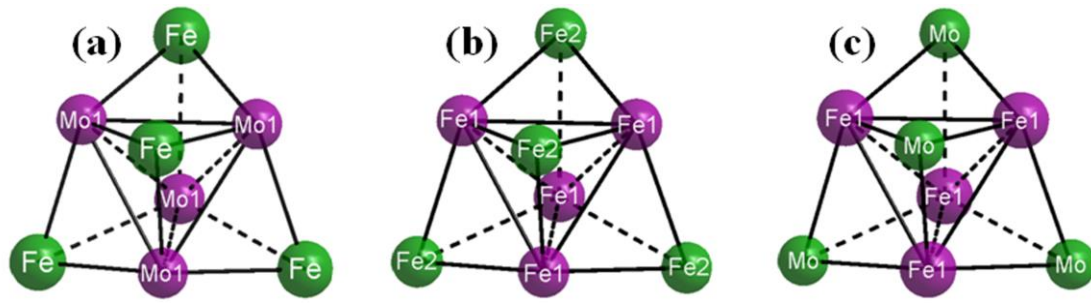


Fig. 5. SQ and pseudo-SQ lattices for alloy carbide $\text{Fe}_{6-x}\text{Mo}_x\text{C}$. Green and purple spheres represent 16d and 32e Wyckoff sites, respectively. (a) Pseudo-SQ lattice of $\text{Fe}_2\text{Mo}_4\text{C}$. Atom Fe and Mo1 sites are indicated in Table 2. (b) SQ lattice of $\text{Fe}_3\text{Mo}_3\text{C}$. The Fe1 and Fe2 sites are $(0.294\ 0.294\ 0.294)$ and $(0.5\ 0.5\ 0.5)$, respectively [18]. (c) Pseudo-SQ lattice of $\text{Fe}_4\text{Mo}_2\text{C}$ carbides. Fe1 and Mo atom sites are $(0.625\ 0.625\ 0.625)$ and $(0.832\ 0.832\ 0.832)$, respectively.

Figure 6

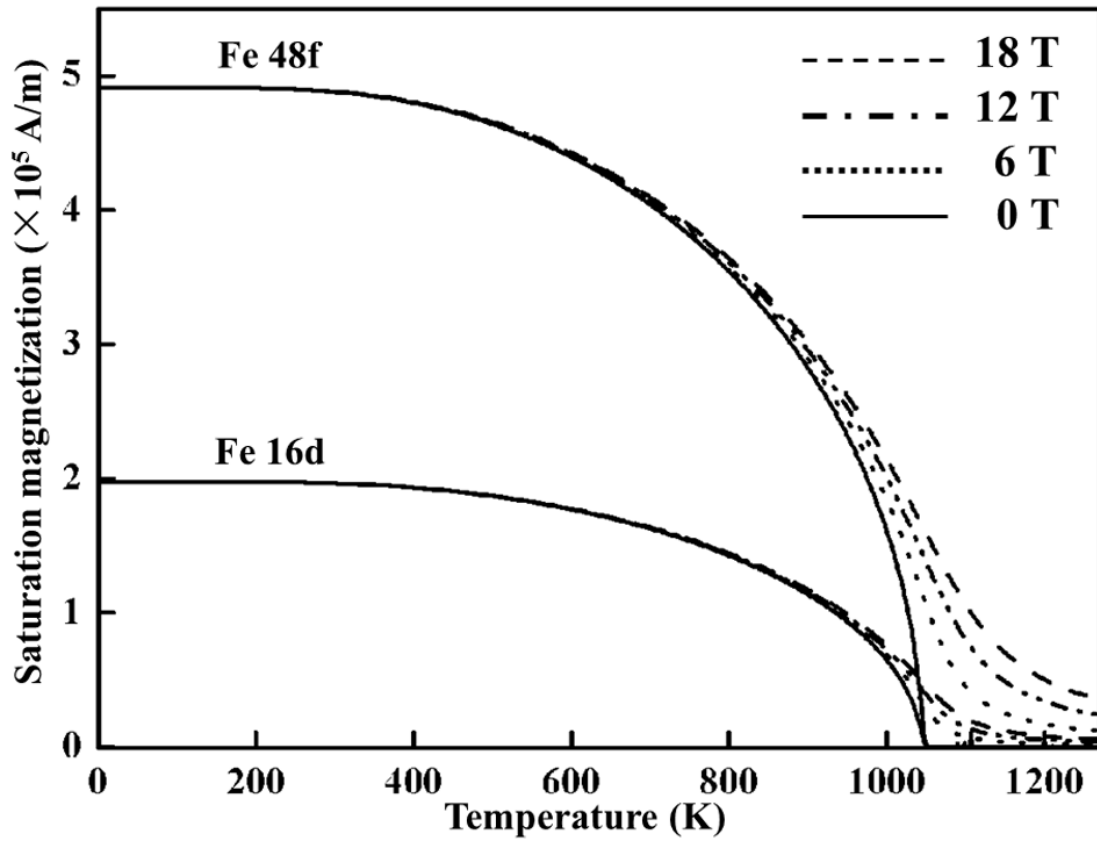


Fig. 6. Variation of saturation magnetization for Fe atom in 48f or 16d sites in the carbide of $\text{Fe}_4\text{Mo}_2\text{C}$ with different temperatures and magnetic field strengths.

Figure 7

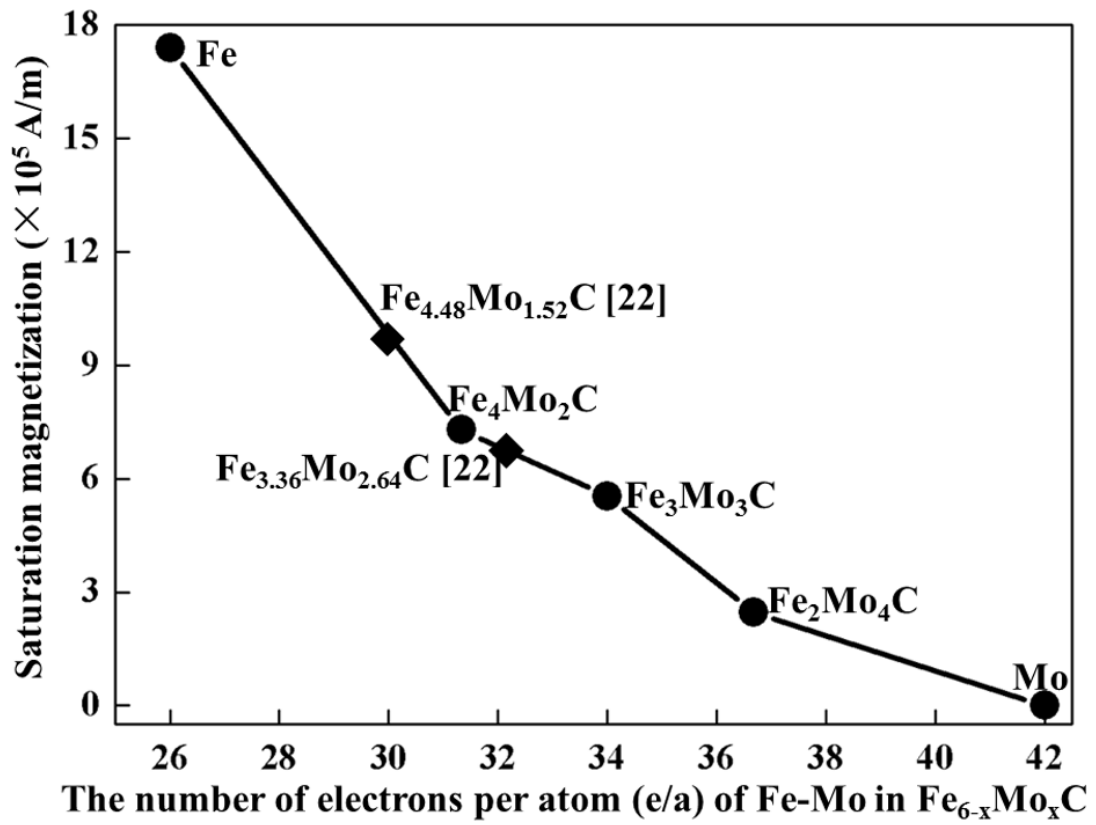


Fig. 7. Variation of saturation magnetization with the number of electrons per atom for the $\text{Fe}_{6-x}\text{Mo}_x\text{C}$ carbides based on the first-principles calculation.

Figure 8

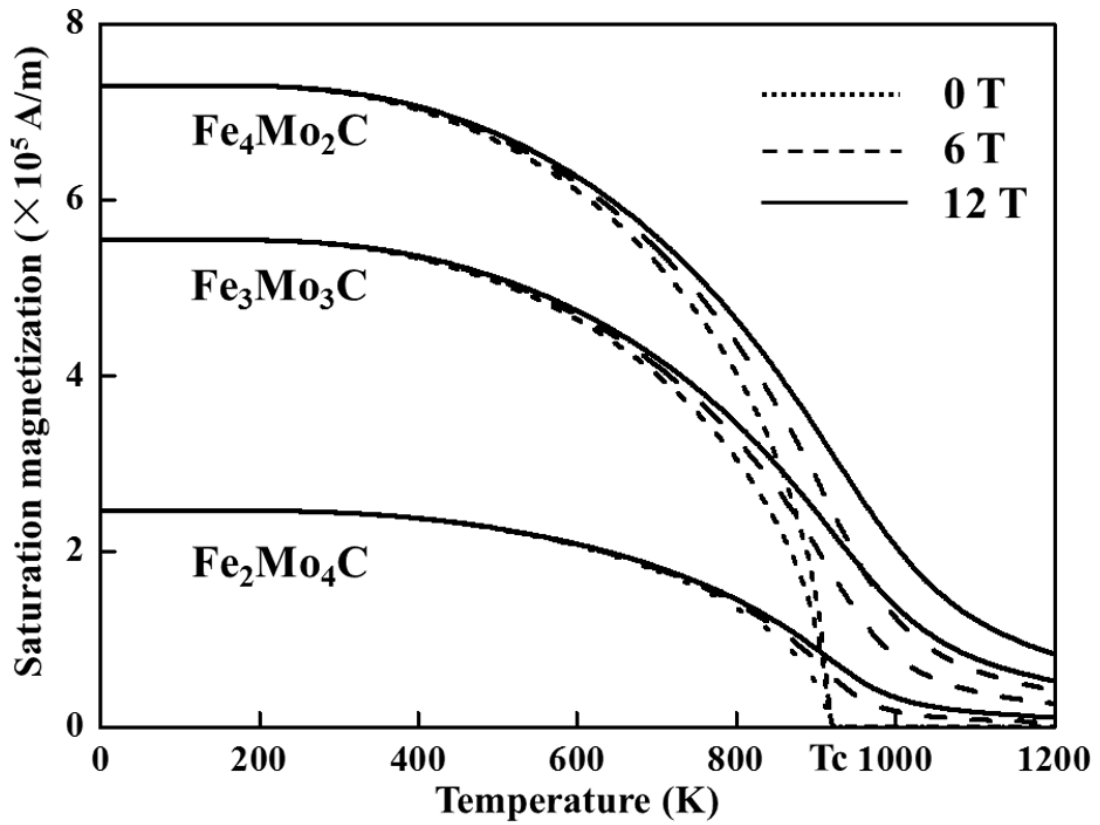


Fig. 8. Temperature variation of saturation magnetization of alloy carbides $\text{Fe}_2\text{Mo}_4\text{C}$, $\text{Fe}_3\text{Mo}_3\text{C}$ and $\text{Fe}_4\text{Mo}_2\text{C}$ with different temperatures and magnetic field strengths.

Figure 9

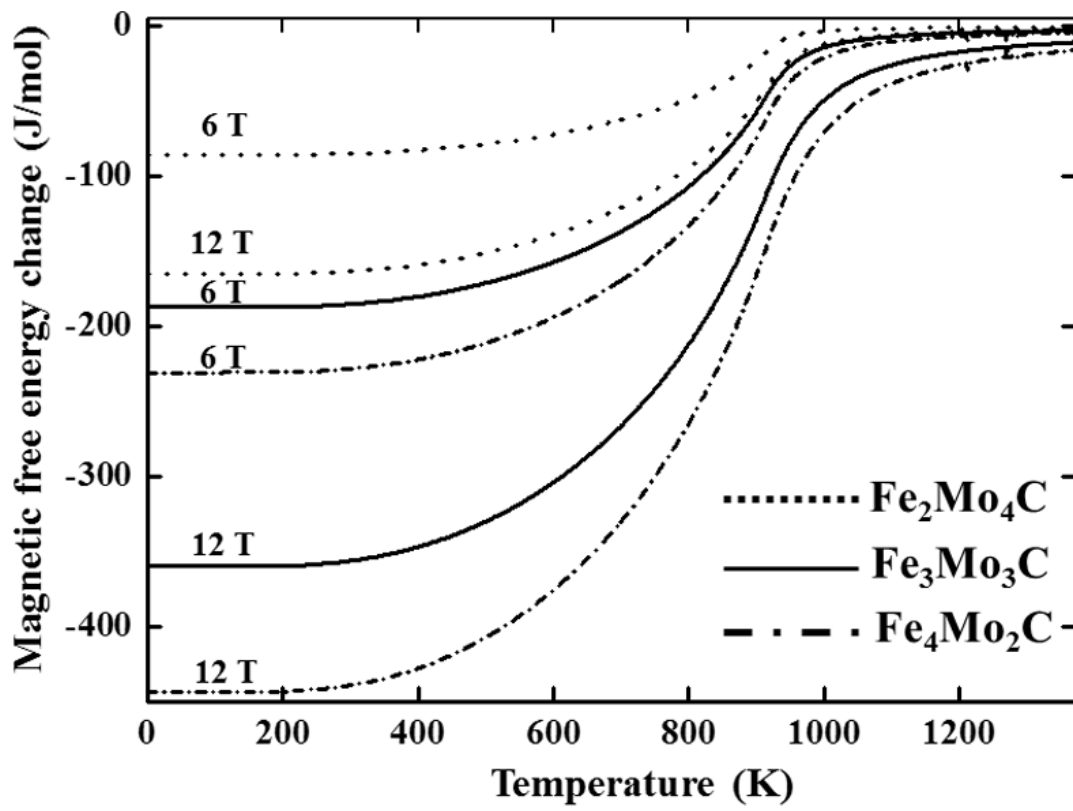


Fig. 9. Magnetic energy change with a 12 T magnetic field strength for alloy carbides Fe₂Mo₄C, Fe₃Mo₃C and Fe₄Mo₂C.

Figure 10

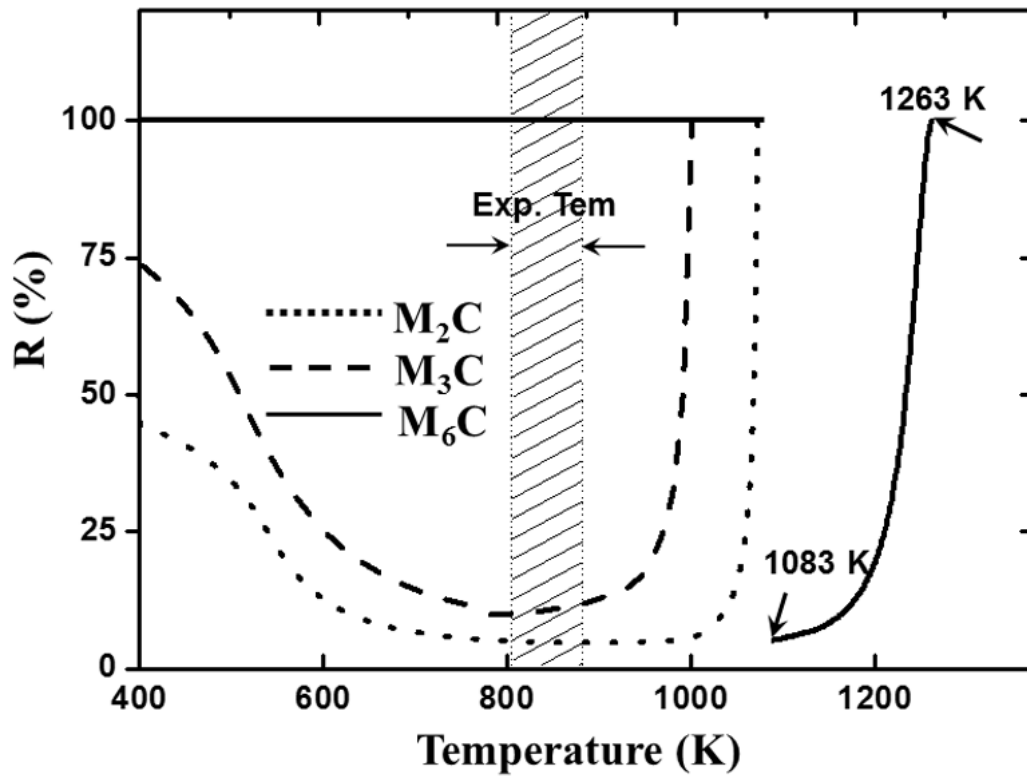


Fig. 10. The ratio of magnetic free energy change to the total free energy change including thermal and magnetic free energy for M_2C , M_3C and M_6C . The shadow area shows the experimental range in Table 1.

Table 1 The carbide type formed in Fe-0.28C-3.0Mo alloy from austenite-to-bainite and during tempering without and with the presence of 12 T magnetic field.

Heat treatment	Ref.	Temperature (°C)	Time (s)	
			B=0 T	B=12 T
			M ₂ C, M ₃ C	M ₂ C, M ₃ C, M ₆ C
Austenite-to-bainite reaction	[8]	570	(20, 60, 600, 3600)	(20, 60, 600, 3600)
	[8]	610	(20, 60, 600)	(60, 600, 3600)
	[21]	530	3600	3600
Tempering	[22]	530	3600	3600

Note: M stands for Fe and Mo atoms.

Table 2 Crystal structure and the calculated magnetic moments (μ_B) of Fe₂Mo₄C.

Space group	Atom	Site	x/a, y/b, z/c	Magnetic moments per Fe atom (μ_B)
$\bar{F}d\bar{3}m$	Fe	32e	(0.832 0.832 0.832)	1.33000
	Mo1	16d	(0.625 0.625 0.625)	-0.09334
	Mo2	48f	(0.198 0 0)	-0.02733
	C	16c	(0.125 0.125 0.125)	0.00047

Table 3 Comparison of the nearest neighbor Fe-C bond distances (\AA) with the magnetic moments of alloy carbides ($\text{Fe}_2\text{Mo}_4\text{C}$, $\text{Fe}_3\text{Mo}_3\text{C}$ and $\text{Fe}_4\text{Mo}_2\text{C}$).

Carbide types	Wyckoff positions	Magnetic moments	Bond distances (\AA)
$\text{Fe}_2\text{Mo}_4\text{C}$	32e	1.33	3.41
$\text{Fe}_3\text{Mo}_3\text{C}$	32e	1.86	3.34
$\text{Fe}_4\text{Mo}_2\text{C}$	48f	2.06	2.12

Table 4 Comparison of the formation temperature without and with the presence of 12 T magnetic field in Fe-C-Mo alloy.

Carbide types	B=0 T	B=12 T	ΔT
M ₂ C	1082.5	1085.5	3
M ₃ C	1003.5	1011	7.5
M ₆ C	1263	1274	11

Note: The calculation of carbide formation temperature assumes that carbides are precipitated from austenite or ferrite. The formation temperature of M₂C M₃C and M₆C in the absence of the magnetic field is obtained by MTDATA.

Table 5 The average ratio (R) of the magnetic free energy with a 12 T field to the total free energy in the experimental range (803~883 K) for M_2C M_3C and M_6C .

Carbide types	R value (%)
M_6C	100
M_2C	4.13
M_3C	8.97